JOURNAL OF GEOPHYSICAL RESEARCH, VOL. 115, G02011, doi:10.1029/2009JG001122, 2010

Climatic controls of interannual variability in regional carbon fluxes from top-down and bottom-up perspectives

Ankur R. Desai,[1] Brent R. Helliker,[2] Paul R. Moorcroft,[3] Arlyn E. Andrews,[4] and Joseph A. Berry[5]

Received 14 August 2009; revised 10 December 2009; accepted 21 January 2010; published 1 May 2010.

[1] Observations of regional net ecosystem exchange (NEE) of CO_2 for 1997–2007 were analyzed for climatic controls on interannual variability (IAV). Quantifying IAV of regional (10^4–10^6 km^2) NEE over long time periods is key to understanding potential feedbacks between climate and the carbon cycle. Four independent techniques estimated monthly regional NEE for 10^4 km^2 in a spatially heterogeneous temperate-boreal transition region of the north central United States, centered on the Park Falls, Wisconsin, United States, National Oceanic and Atmospheric Administration tall tower site. These techniques included two bottom-up methods, based on flux tower upscaling and forest inventory based demographic modeling, respectively, and two top-down methods, based on tall tower equilibrium boundary layer budgets and tracer-transport inversion, respectively. While all four methods revealed a moderate carbon sink, they diverged significantly in magnitude. Coherence of relative magnitude and variability of NEE anomalies was strong across the methods. The strongest coherence was a trend of declining carbon sink since 2002. Most climatic controls were not strongly correlated with IAV. Significant controls on IAV were those related to hydrology, such as water table depth, and atmospheric CO_2. Weaker relationships were found with phenological controls such as autumn soil temperature. Hydrologic relationships were strongest with a 1 year lag, potentially highlighting a previously unrecognized predictor of IAV in this region. These results highlight a need for continued development of techniques to estimate regional IAV and incorporation of hydrologic cycling into couple carbon-climate models.

Citation: Desai, A. R., B. R. Helliker, P. R. Moorcroft, A. E. Andrews, and J. A. Berry (2010), Climatic controls of interannual variability in regional carbon fluxes from top-down and bottom-up perspectives, *J. Geophys. Res.*, *115*, G02011, doi:10.1029/2009JG001122.

1. Introduction

[2] Observations of regional (10^4–10^6 km^2) surface-atmosphere carbon net ecosystem exchange (NEE) can be related to underlying biome types, coherent climate forcings, and land use and disturbance patterns, and thus are key to facilitating mechanistic understanding of drivers of carbon fluxes [*Running*, 2008]. Regions are also the scale of impact for global climatic change and a relevant scale for land management and CO_2 emission decisions [*Wofsy and Harriss*, 2002]. However, observations of regional carbon exchange have been limited [*Desai et al.*, 2008; *Dolman et al.*, 2009; *Riley et al.*, 2009].

[3] Regions often contain multiple ecosystem types, heterogeneous terrain, and developed areas. As such, it is difficult to scale up from ecosystem-based studies to the region [*Desai et al.*, 2008] and the regional complexity complicates scaling down from global-scale flux estimates based on atmospheric approaches [*Ahmadav et al.*, 2009; *Gurney et al.*, 2002]. Thus, "top-down" carbon cycle observations have traditionally been limited to the continental scale (~10^7–10^8 km^2) while "bottom-up" methods to the scale of a local ecosystem (~10^0–10^1 km^2).

[4] Quantifying regional NEE and how it varies with climate drivers can help improve prediction of carbon cycle–climate feedbacks, of which there are many [*Bonan*, 2008]. Though progress has been made in capturing many of these processes [*Moorcroft*, 2006], uncertainty in carbon cycle climate sensitivity continues to remain a significant source of uncertainty in the trajectory of future climate change [*Friedlingstein et al.*, 2006]. Some of this uncertainty could be diagnosed by better understanding of the interannual variability of atmospheric CO_2, which is strongly driven by

[1]Department of Atmospheric and Oceanic Sciences, University of Wisconsin-Madison, Madison, Wisconsin, USA.
[2]Department of Biology, University of Pennsylvania, Philadelphia, Pennsylvania, USA.
[3]Department of Organismic and Evolutionary Biology, Harvard University, Cambridge, Massachusetts, USA.
[4]Earth System Research Laboratory, National Oceanic and Atmospheric Administration, Boulder, Colorado, USA.
[5]Carnegie Institution of Washington, Stanford University, Stanford, California, USA.

0148-0227/10/2009JG001122

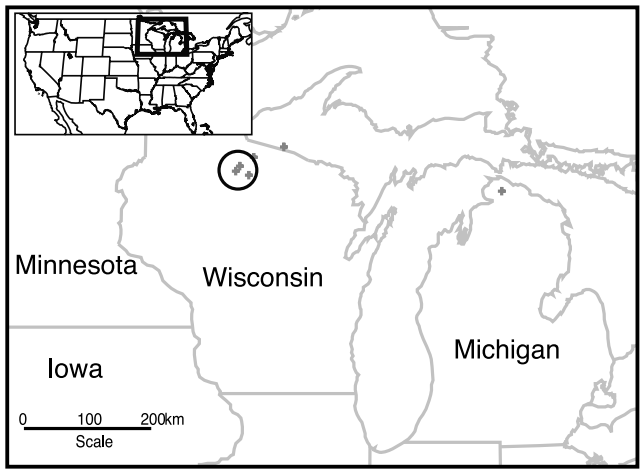

Figure 1. Map of region (inset at top left) including location of eddy covariance flux towers used by IFUSE model (gray crosses) and delineation of bottom-up region upscaling region (black circle), a 60 km radius circle around the Park Falls, Wisconsin, United States, WLEF tall tower NOAA greenhouse gas observatory site.

climatic processes. The variability of CO_2 at annual to decadal timescales is driven primary by interannual variability (IAV) of terrestrial carbon cycle [*Bousquet et al.*, 2000; *Peylin et al.*, 2005]. Yet, diagnosing climate controls on terrestrial IAV is not simple [*Law et al.*, 2002; *Ricciuto et al.*, 2008].

[5] Despite these difficulties, there is much potential in ongoing long-term carbon cycle observations to better constrain regional NEE and its climate controls. The proliferation of eddy covariance flux towers, carbon inventories, and continuous atmospheric CO_2 observations, coupled with advances in top-down and bottom-up scaling methods has great potential to better improve quantification of regional NEE and its IAV [*Pacala et al.*, 2001]. Bottom-up methods have generally incorporated ecosystem and scaling models applied to flux chambers [*Kicklighter et al.*, 1994], flux towers [*Desai et al.*, 2008; *Papale and Valentini*, 2003; *Xiao et al.*, 2008], carbon inventories [*Cohen et al.*, 1996; *Desai et al.*, 2007; *Goodale et al.*, 2002], or satellite remote sensing [*Mahadevan et al.*, 2008]. Top-down methods have primary focused on aircraft atmospheric budgets [*Leuning et al.*, 2004; *Lin et al.*, 2004; *Matross et al.*, 2006], tower based boundary layer observations [*Bakwin et al.*, 2004; *Chen et al.*, 2007; *B. Chen et al.*, 2008; *Denmead et al.*, 1996; *Helliker et al.*, 2004; *Kuck et al.*, 2000; *Levy et al.*, 1999; *Wang et al.*, 2007], or tracer-transport inversion [*Gurney et al.*, 2002; *Peters et al.*, 2007]. Very few studies [e.g., *Pacala et al.*, 2001; *Riley et al.*, 2009] combine multiple methods or attempt to assess carbon fluxes over multiple years, limiting much of the inference drawn from any one method about controls on regional IAV.

[6] To fully investigate magnitude and IAV of regional NEE, multiple top-down and bottom-up methods need to be investigated [*Blankinship et al.*, 2008]. In this study, we apply four independent methods, two bottom-up, two top-down to estimate regional NEE for a 10 year period (1997–2007) over a small region (10^4 km^2) located in the upper Midwest United States in a boreal transition region. The wetland-interspersed forested landscape drives complex spatial heterogeneity.

[7] The region is centered on the WLEF Park Falls, Wisconsin, United States, tall tower site, where a decade of atmospheric greenhouse gas [*Bakwin et al.*, 1998], eddy covariance flux tower [*Davis et al.*, 2003], inventory [*Bolstad et al.*, 2004], and regional climatic observations [*Ricciuto et al.*, 2008] have been made. Four independent methods were analyzed for regional NEE, IAV, and relationship of IAV to climatic variables. The methods include a flux tower upscaling study [*Desai et al.*, 2008; A. R. Desai, Climate and phenology drive coherent regional interannual variability of carbon dioxide flux in a heterogeneous landscape, submitted to *Journal of Geophysical Research*, 2010], an inventory based ecosystem model [*Desai et al.*, 2007; *Moorcroft et al.*, 2001], an equilibrium tower-based boundary layer budget [*Helliker et al.*, 2004], and a tracer-transport inversion [*Peters et al.*, 2007]. This study extended original studies of these methods to the entire time period and attempted to estimate uncertainty for them.

[8] Given monthly NEE and annual IAV from the four methods, we asked: (1) Is there convergence in the magnitude of mean NEE and the timing of the seasonal cycle and if not, how might these differences be reconciled in terms of model structure? (2) How coherent is IAV across the four methods and are there any consistent anomalies and trends? (3) What environmental and climatic controls best explain any coherent IAV?

2. Methods

2.1. Region Description

[9] Regional carbon fluxes and climatic variables were examined in a 60 km radius of the WLEF tall tower (45°56′N, 90°16′W) near Park Falls, Wisconsin, United States (Figure 1). The region is a subboreal forested landscape, with low human population density and little elevation change [*Desai et al.*, 2007]. The dominant cover of mature and young northern hardwoods is interspersed with softwood stands and forested and open wetlands. Most of the forest is managed, though harvest only occurs in limited parts of the region currently [*Ahl et al.*, 2005]. The complexity of the landscape in ecosystem types, ages, management class, and stocking is the precisely the reason that regional carbon fluxes are difficult to quantify by any one method.

[10] The climate is characterized by cold winters, warm, short summers, and moderate precipitation amounts. The mean annual temperature over the time period examined (1997–2006) was 6.0 +/− 1.1 C with a range from −6.5 +/− 1.9 C in winter (December–February) to 18.0 +/− 1.1 C insummer (June–August). Mean precipitation was 723 +/− 128 mm, with 58 +/− 6% falling from May–September, and most winter precipitation falling as snow. Forests productivity in the region is generally considered to be primarily temperature limited, and relatively insensitive to variations in precipitation.

2.2. Regional Flux Techniques

2.2.1. Materials

[11] The time period examined was January 1997 to December 2006. This period overlaps with high-quality observations of greenhouse gases, eddy covariance carbon

Table 1. Definitions of the Bottom-Up and Top-Down Regional Flux Methods and Climatic Variables Used in This Study

	Name	Citation
Bottom-up		
IFUSE	Interannual Flux Tower Upscaling Experiment	A. R. Desai et al. (manuscript in preparation, 2010)
ED	Ecosystem Demography Model v. 1.5	*Desai et al.* [2007]
Top-down		
EBL	Equilibrium Boundary Layer budgets	*Helliker et al.* [2004]
CT	CarbonTracker inverse model, version 2008	*Peters et al.* [2007]
Variable		
T_{air}	air temperature (30 m)	
T_{soil}	soil temperature (10 cm)	
PAR	photosynthetically active radiation	
Precip	Precipitation	
VPD	vapor pressure deficit	
Q_{soil}	soil moisture (10 cm)	
Q_{table}	water table depth above surface	
$[CO_2]$	atmospheric carbon dioxide concentration	
NAO	North Atlantic Oscillation index	
NINO3.4	El Nino 3.4 index	
PNA	Pacific North-America Oscillation index	

dioxide fluxes, and regional micrometeorology from a network of observations that are within the Chequamegon Ecosystem Atmosphere Study (ChEAS) [*J. Chen et al.*, 2008; *Davis et al.*, 2003]. The WLEF tall tower is instrumented by the National Oceanic and Atmospheric Administration (NOAA) Earth Systems Research Lab (ESRL) for continuous monitoring of atmospheric greenhouse gases since 1995 [*Bakwin et al.*, 1998].

[12] Continuous vertical profiles of atmospheric CO_2 ($[CO_2]$) and meteorological variables are measured at the WLEF tall tower and used in this analysis for the boundary layer budgets, atmospheric inversions, and inference of mean atmospheric state. $[CO_2]$ observations, made at 6 heights from the tower and aggregated to hourly averages, have an accuracy of +/− 0.2 ppm. Hourly average meteorological profiles include temperature and humidity at three levels and surface incoming radiation variables. Missing meteorological data were gap−filled with a nearest neighbor approach using other meteorological stations in the region.

[13] Since the initiation of greenhouse gas monitoring, additional micrometeorological and stand-scale eddy covariance flux towers in forests and wetlands have been installed across the landscape (Figure 1) [*Desai et al.*, 2008]. These micrometeorology towers provided soil moisture and temperature observations in addition to atmospheric variables. The eddy covariance towers directly measured exchange of trace gas fluxes at the scale of ~1 km^2. NEE, the direct exchange of CO_2, was observed by all towers at half-hourly resolution. Data gaps were filled using conventional empirical regression techniques [*Desai et al.*, 2005].

[14] Other data required for the methods include biological measurements of species composition, land cover, and standing carbon stocks, which have been made across the region in a number of investigations [*Bolstad et al.*, 2004]. Distribution of forest age and biomass was derived from the U.S. Forest Service Forest Inventory and Analysis (FIA) program, which sampled tree species, height, age, and other variables in stratified random plots at decadal intervals. We selected FIA plots in a 60 km^2 radius around the WLEF tower and used converted these data into statistics of forest age-class biomass distributions.

[15] Various combinations of these $[CO_2]$, meteorological, eddy flux, soil state, and species composition data sets are required by the four regional carbon flux methods. These methods are described in the next four sections and also noted in Table 1. Two of the methods are "bottom-up" as they rely on upscaling a network of ecosystem observations to a region using a mapping of point to area and two of the methods are "top-down" as they rely on inferring entire region flux from atmospheric observations.

2.2.2. Bottom-Up Technique: IFUSE

[16] Building on an upscaling experiment described by *Desai et al.* [2008], the Interannual Flux Tower Upscaling Experiment (IFUSE) regional carbon ecosystem approach (Desai, submitted manuscript, 2010) is a simple, data assimilation based approach to estimating regional carbon fluxes from a mesonet of eddy covariance flux towers. Direct observations of surface-atmosphere exchange of CO_2 measured by eddy covariance flux towers were used to calibrate a simple ecosystem model, which was then applied to an upscaling model to calculate regional sources and sinks of carbon in forests and wetland ecosystems (Desai, submitted manuscript, 2010). Unlike *Desai et al.* [2008], IFUSE estimates regional fluxes for the entire year and is designed to preserve observed interannual variability.

[17] IFUSE's ecosystem model is a minimal-parameter (17), spin-up free model of ecosystem photosynthesis and respiration. The diagnostic model has no soil pools, and thus assumes they are fixed in time relative to variations in fluxes, which reduces the difficulty of parameter estimation for turnover times but limits the ability of the model to be run at successional timescales. Calibration against flux towers allows the model to successfully simulate ecosystem carbon exchange and impact of climate variability on them.

[18] Half-daily (day/night) estimates of gross primary production, ecosystem respiration, NEE, and leaf area index are output. Photosynthesis is estimated using an eight-parameter light, temperature, and vapor pressure deficit limited Montieth model. Five parameters control respiration rates in three temperature, production, and moisture sensitive soil pools. Leaf phenology is modeled with a four-parameter sigmoidal growing degree day and soil temperature sensitive function for leaf emergence and leaf fall, respectively. While the model is purposefully simple and primarily designed for forests, we assume that wetlands and nonforest ecosystems generally follow the same relationships in the bulk and rely on the calibration to flux tower data to constrain the parameters for these ecosystems.

[19] NEE observations from the ChEAS flux tower network were used to calibrate 14 of the 17 parameters in the model using a hierarchical Bayesian approach [*Luo et al.*, 2009]. More than one dozen flux towers were used, which spanned the range of age classes (young, intermediate, mature, old growth) and land covers (mixed forest, evergreen needleaf forest, and wetland) seen in the region, though some (e.g., mature forests) were oversampled compared to others (e.g., wetlands).

[20] We used the Markov Chain Monte Carlo (MCMC) Metropolis-Hastings algorithm [*Braswell et al.*, 2005;

Metropolis and Ulam, 1949] to estimate the posterior distribution of parameters for each flux tower site, as described in detail by Desai (submitted manuscript, 2010). The MCMC approach and the ecosystem model were applied to each tower to estimate optimal parameter distributions that best explain daily and interannual variations of carbon fluxes at the site. A simple approach (based on *Desai et al.* [2008]) was then used to scale the modeled NEE at the individual flux towers to the region, based on how representative each site was of each land cover and forest age class in the region. Land cover maps were derived from high-resolution satellite analysis. Stand age distribution was derived from the U.S. Forest Service Forest Inventory Analysis (FIA). Finally, the meteorological forcing data were applied and mean NEE were proportionally summed to estimate region daily NEE from 1997 to 2006.

[21] Uncertainty due to errors in meteorological forcing, model parameters, and distributions of land cover was assessed by running the model with 1,000 random perturbations in these three error types. For meteorology, uniform random errors of 1°C in temperatures and 10% in PAR and VPD were assumed. For parameter uncertainty, parameter sets from the posterior distribution were randomly sampled and applied to the model. For land cover, 10% uniform random errors in the amount of land cover for each type were assumed. These three uncertainty tests were applied jointly and provide a conservative estimate of the random error in the estimate flux, but do not sample systematic errors of how representative the towers and models are for estimating regional flux. *Desai et al.* [2008] showed incorporation of wetland and young forest flux tower data significantly impacts estimates of regional flux. Here we assume that each land cover is adequately sampled by the flux towers.

2.2.3. Bottom-Up Technique: ED

[22] The Ecosystem Demography (ED) model is a height-and-age structured ecosystem model, originally applied to predict ecosystem structure and function in the Amazon [*Moorcroft et al.*, 2001]. ED is a dynamic ecosystem model that explicitly models plant functional type (PFT) based height structured competition and stochastic disturbance by keeping track of changes in statistical distributions of subgrid variations in patch age and PFT cohort heights due to growth, mortality, and disturbance. Subsurface biogeochemistry is modeled using a multiple soil pool and turnover time approach [*Moorcroft et al.*, 2001]. A North American parameterized version of ED [*Albani et al.*, 2006] was modified and calibrated for use in the ChEAS region [*Desai et al.*, 2007].

[23] The ED model in ChEAS was primarily calibrated by species composition, height, and age information derived from FIA and run forward with both climatic forcing derived from meteorological observations and disturbance forcing parameterized with known rates of forestry, land clearing, and natural disturbance. The version for ChEAS was parameterized independently for northern hardwoods stands, conifer softwood stands, and forested wetlands. The model was initialized with near-equilibrium carbon pools in 1800 and run forward with potential vegetation based on nineteenth century vegetation survey data until 1850 when land use change is enacted. Because of the nature of ED age and cohort structure, long spin-up is not needed as detailed by *Desai et al.* [2007]. Carbon pools in ED were in close agreement to those observed in the field at flux tower sites [*Desai et al.*, 2007].

[24] Land cover fractions were used to sum regional flux from the runs for each ecoregion type (deciduous, conifer, and wetland). Results from this model compared well to NEE observed by the flux tower network. All ecosystems were fed the same climate data derived from the WLEF tower meteorology. The wetland run simulated wetland hydrology by increasing precipitation, but was otherwise treated like a forest with wetland plant species parameterizations.

[25] Two additions were made to ED in this paper compared to *Desai et al.* [2007]. First, the model was run forward in time to 2006 instead of ending in 2004. Second, uncertainty in regional NEE from ED due to uncertainty in age and cover distribution was estimated. Errors of 10% in age distribution and 10% in land cover were randomly applied to 1,000 iterations of the ED model output. The resulting output was used to compute mean and standard deviation in regional NEE for each month.

2.2.4. Top-Down Technique: EBL

[26] The mixing ratio of CO_2 in the atmospheric boundary layer (ABL) is a reflection of surface fluxes and meteorological processes which tend to mix free-tropospheric air into the ABL [*Raupach et al.*, 1992]. Continuous measurements of CO_2 in the continental ABL from tall towers are more strongly influenced by surface-flux effects on atmospheric CO_2 as compared to 'background' marine boundary layer measurements [*Bakwin et al.*, 1998]. Reasonable estimates of regional surface CO_2 flux can be obtained by inverting CO_2 budgets of the convective boundary layer during the period of daytime, nonlinear ABL growth [*Denmead et al.*,1996; *Levy et al.*, 1999; *Kuck et al.*, 2000; *Lloyd et al.*, 2001; *Styles et al.*, 2002]. However, quantifying fair-weather cloud flux, entrainment, subsidence and horizontal divergence over a day is problematic and often results in poor agreement between ABL budget methods and surface-based methods [*Cleugh et al.*, 2004].

[27] *Helliker et al.* [2004] recognized that over long enough timescales, the mean difference between the mixing ratio of CO_2 in the ABL and in the free troposphere, together with an estimate of vertical mixing, could be used to estimate surface fluxes. This equilibrium boundary layer (EBL) approach [*Betts et al.*, 2004] was successfully applied to resolve monthly NEE over 1 year by *Helliker et al.* [2004] and *Bakwin et al.* [2004]. The budget equation for CO_2 in the steady state ABL can be written as [*Helliker et al.*, 2004; cf. *Raupach et al.*, 1992; *Denmead et al.*, 1996; *Levy et al.*, 1999; *Kuck et al.*, 2000; *Lloyd et al.*, 2001; *Styles et al.*, 2002],

$$\rho h \partial C_m / \partial t = NEE - \rho W (C_t - C_m), \quad (1)$$

where C is the mean CO_2 mixing ratio, subscripts m and t refer to ABL (mixed layer) and free troposphere, respectively, and NEE is the net surface flux of CO_2. ρ is density, h is ABL height. $W = \partial h/\partial t - W^*$ is the rate at which ABL air mixes with free tropospheric air. W* represents the mean subsiding flow. Over longer averaging periods of fair-weather days, $W \rightarrow W^*$ and is typically negative corresponding to mean, large-scale subsidence. Stormy periods, defined here by a 24 h period where greater than 1 mm of precipitation is recorded, represent about 23% of

days annually at the study site [*Helliker et al.*, 2004]. Free troposphere CO_2 was estimated based on same latitude marine boundary layer values available from the NOAA ESRL GLOBALVIEW time-interpolated flask CO_2 data set.

[28] To solve for the regional surface flux of CO_2, equation (1) is rearranged as,

$$NEE = \rho W(C_t - C_m) + \rho h \partial C_m / \partial t \quad (2)$$

Helliker et al. [2004] show that the storage term, $\rho h \partial Cm/\partial t$, can become very small over monthly timescales. Thus, under a strict steady state or equilibrium assumption, the storage term becomes zero and equation (2) reduces to:

$$NEE = \rho W(C_t - C_m). \quad (3)$$

The overriding challenge for solving for NEE in equations (2) and (3) is finding long-term estimates of the effective mixing velocity ρW. A modeled representation of ρW is available from weather model reanalysis. Estimates of ρW at 700 hPa were obtained from the 24 h daily average pressure vertical velocity (Ω; Pa s^{-1}) of the NOAA North American Regional Reanalysis (NARR), by

$$\rho W = -\Omega / g \quad (4)$$

where Ω is vertical pressure velocity (Pa s^{-1}) and g is gravitational acceleration.

[29] It was further determined that a period of integration for equation (3) of 14 days was short enough to resolve CO_2 flux responses to synoptic-scale weather events, yet long enough for the ABL to be at or near equilibrium [*Hurwitz et al.*, 2004]. Using this period of integration (averages of ρW, C_t, and C_m for fair-weather conditions), reasonable estimates of net regional CO_2 flux were obtained for the entire time period at the WLEF tall tower.

[30] Although prior studies have suggested that the systematic error (e.g., fair-weather bias) may limit the ability of EBL-like techniques to accurately estimate annual fluxes [e.g., *Leuning et al.*, 2004], *Helliker et al.* [2004] showed that with careful selection of precipitation screening criteria and proper long-term averaging of mixing ratio data, the EBL technique could reasonably estimate monthly flux. Additionally, multiyear analysis of vertical velocity averaging times showed that 14 day averages adequately captured enough synoptic mixing events. With these criteria applied, EBL had good agreement with NEE measured by the WLEF tall tower eddy covariance flux and also compared well to a full solution of equation (1) during a period when boundary layer height estimates are available. This study extends the 1 year analysis of *Helliker et al.* [2004] to the entire time period. Additionally, uncertainty in NEE from this method was assessed by randomly perturbing 20% errors in ρW, and 0.5 ppm error in both ABL and free troposphere CO_2 and recomputing NEE 1000 times.

2.2.5. Top-Down Technique: CT

[31] CarbonTracker (CT) is a global inverse model for CO_2 flux developed by NOAA ESRL [*Peters et al.*, 2007]. The method relies on atmospheric CO_2 observations from the NOAA ESRL Cooperative Air Sampling network, including those monitored at the NOAA WLEF greenhouse gas observatory. These observations, along with modeled transport fields and an ecosystem model are used in data assimilation mode to estimate ecosystem parameters that optimize model to data difference of atmospheric CO_2.

[32] The transport model is a nested grid model with a higher resolution (1° × 1°) over the United States. Fossil fuel and fire CO_2 fluxes were prescribed from existing databases, and land and oceanic fluxes were adjusted to match the atmospheric CO_2 observations. The land is divided into 25 ecoregions based on continent and land cover, while the oceans are divided into 11 basins. The optimization approach adjusted weekly linear scaling factors for each basin or ecoregion using an Ensemble Kalman Filter approach [*Peters et al.*, 2005]. Prior land fluxes were prescribed at 3-hourly time resolution from the Carnegie Ames Stanford Approach (CASA) ecosystem model. Weather model and satellite vegetation greenness information drove the biosphere fluxes of CASA, while the linear scaling factor adjusted the flux scaling for each ecoregion based on the atmospheric constraint.

[33] While CT was designed to estimate fluxes at the continental scale, variability in small region fluxes will still be reflected the information content of near-field atmospheric CO_2. Here, we extracted CT, release 2008, surface biosphere fluxes from 2000 to 2006 for the WLEF region, which are likely to be strongly sensitive to CO_2 observed at the WLEF tower. While the short-term variations in CT primarily represent the processes in the CASA model, the magnitude and interannual variability of these fluxes are reflective of the atmospheric CO_2 constraint. The output provided from CT provided NEE estimate at a 3-hourly time step. No approach to estimate uncertainty was taken here.

2.3. Analysis of Environmental Controls

2.3.1. Climate Data

[34] We compared estimated regional NEE from the four methods to a number of different climate variables (Table 1). These variables include atmospheric, subsurface, and climate index variables. Atmospheric values such as air temperature (T_{air}), vapor pressure deficit (VPD), photosynthetic active radiation (PAR), precipitation (Precip), atmospheric [CO_2] were derived from the WLEF tall tower meteorological sensors, with gaps filled by regression against nearest neighbor meteorological stations. Forest micrometeorology station data were averaged and used to develop time series of subsurface 10 cm soil temperature (T_{soil}) and moisture (Q_{soil}). Water table depth (Q_{table}) was observed at the Lost Creek shrub wetland [*Sulman et al.*, 2009] using a pressure transducer system from 2001 to 2006. To infer prior year values, we found a strong fit of Q_{table} to nearby bog water level sampling ($r^2 = 0.90$) from the North Temperate Lakes Long-term Ecological Research (LTER) Crystal bog site. These data allowed us to extrapolate Q_{table} for the entire period of interest. Finally, climate index values for North Atlantic Oscillation (NAO), El Nino (NINO3.4), and Pacific North-America Oscillation (PNA) that may explain interannual variability were retrieved from NOAA Climate Prediction Center. Monthly and seasonal (December–February is DJF, March–May is MAM, July–August is JJA, and September–November is SON) averages and anomalies were computed for each variable.

2.3.2. Statistical Analysis

[35] The goal of this analysis was to understand what climate factors explained observed interannual variability

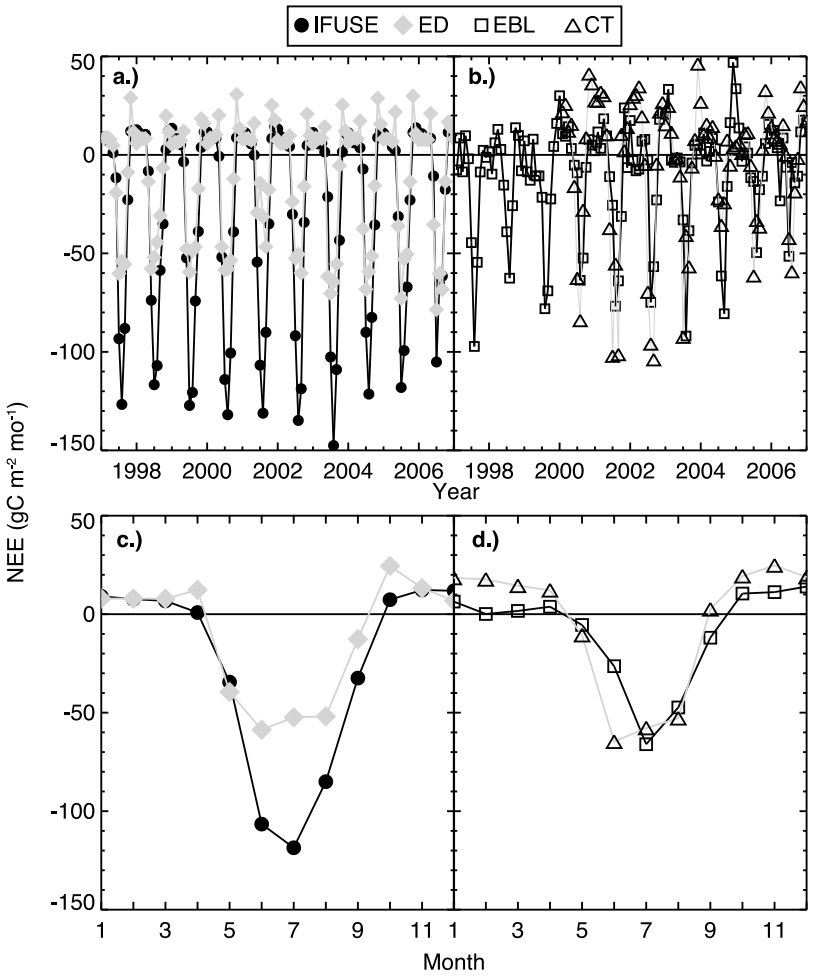

Figure 2. Monthly NEE from the four methods across the entire time record (1997–2006) for the (a) top-down and (b) bottom-up methods and ensemble averaged across all years for (c) "top-down" and (d) "bottom-up. " IFUSE model shows large uptake in the growing season. Both bottom-up methods show more uptake in the spring and autumn.

(IAV) in NEE observed in each of the four methods. Univariate correlation analysis of climate variables against IAV was used to identify strong candidate climate variables (Table 1). In addition to annual climate variables, we also compared IAV to seasonal climate variables. Finally, both annual and seasonal climate variables were lagged by 12 months to test for potential for any predictive climate variables and lagged environment effects on IAV. The strongest predictors of IAV were combined using multivariate linear regression analysis. Interactive effects of predictors were also considered in the multivariate model.

3. Results

3.1. Seasonal Variability

[36] All four methods show strong consistency in patterns of monthly NEE across the entire decade studied (Figure 2, top). Year-to-year variability in peak uptake is strongly consistent, especially among the top-down methods (Figure 2b). A particularly strong pattern of declining peak uptake from 2003 to 2006 is seen in all four methods. In contrast, less consistency is seen in peak winter fluxes, which are typically a source to the atmosphere.

[37] Generally, the mean monthly pattern of NEE among the methods is consistent, though magnitudes in peak autumn emission and summer uptake vary. The IFUSE method shows the largest uptake in the summer months, while the other three methods are nearly half the magnitude (Figure 2, bottom). The CT method has the highest winter NEE, which is sustained from the prior autumn, whereas the other methods show a decline in NEE from autumn into winter. EBL has the lowest winter emissions, especially in late winter.

[38] The bottom-up methods have a longer carbon uptake period, defined as the length of time of negative daily NEE, than the top-down methods, especially CT. The increased uptake period corresponds mostly to large uptake in the start of the growing season (May) than in the autumn. Into the summer, all four methods show a consistent pattern of peak NEE in July, followed by a steady decline in NEE into October.

Table 2. Mean Annual and Growing Season NEE and 1-σ Uncertainty as Described in the Methods, Standard Deviation of IAV, and Correlation Coefficients of Annual NEE Among the Methods[a]

Method	Annual NEE (gC m^{-2})	May–September NEE (gC m^{-2})	IAV (gC m^{-2})	IFUSE	ED	EBL	CT
IFUSE	−321 +/− 13	−377 +/− 12	62		−0.24	0.45	0.53
ED	−135 +/− 5	−215 +/− 5	35	−0.24		−0.23	−0.55
EBL	−110 +/− 14	−157 +/− 12	52	0.45	−0.23		0.84
CT	−58	−183	55	0.53	−0.55	0.84	

[a]IAV is larger than uncertainty for all methods. IFUSE, EBL, and CT are positively correlated to varying degrees, while ED has an opposite pattern. Top-down methods have stronger agreement.

3.2. Interannual Variability

[39] Not surprisingly, given Figure 2, IFUSE has the largest annual and growing season uptake among the three methods (Table 2). Mean NEE differs significantly from the other three, when compared against the 1-σ estimate of uncertainty. ED and EBL have similar annual NEE, but ED shows significantly larger growing season (May–September) uptake, while EBL shows smaller winter NEE. CT has the smallest uptake, but has larger uptake in the growing season than EBL, reflective of the high winter NEE observed in CT (Figure 2d).

[40] The 1-σ interannual variability of NEE ranges from 35 to 62 gC m^{-2} yr^{-1} across the four methods (Table 2), with ED showing the smallest, and the other three methods more similar. While the magnitude of IAV is similar, the correlation matrix in Table 2 reveals significant disagreement among the methods in year-to-year variability of NEE. While IFUSE, EBL and CT are positively correlated to each other, they are all negatively correlated to ED. IFUSE is positively correlated to EBL and CT, but the relationship is weak compared to the correlation among the top-down methods, potentially reflecting the similarly in data source in the two methods.

[41] The differences in NEE magnitude and coherence are further revealed graphically (Figure 3a). The bottom-up methods show greater annual uptake than the top-down methods in a majority of the years, while patterns of coherence vary across the time period. From 1997 to 1999, the bottom-up methods both show a trend of increasing uptake, while EBL trends are more variable and opposite in direction. CT NEE is not available prior to 2000. From 2000 to 2001, the bottom-up methods reverse trend, and show a decline in uptake in 2001, followed by more uptake in ED but no change in IFUSE in 2002. These changes are potentially reflective of the effects of a large pest outbreak in 2001. However, the top-down methods both show an increase in uptake in 2000 to 2001, followed by a decline in 2002.

[42] Coherence in IAV among the methods increases after 2002. From 2002 to 2003, all methods except CT show a slight increase in uptake, while CT shows virtually no change. After 2003, all four methods agree on a relatively larger decline in uptake in 2004 and very little change in 2005. Finally, all except ED continue to show a decline in uptake into 2006, while ED shows an increase.

[43] From an anomaly (deviation from long-term mean NEE) based perspective (Figure 3b), a stronger pattern of consistency is seen. There is coherence in the sign of the NEE anomaly in at least three of four methods in 1998–2001 and 2003–2006. The strongest of these are 1998, 2003, and 2005, perhaps reflective of strong climate forcing anomalies in those three years compared to other years.

3.3. Climatic Controls

[44] Climatic variables tested all show typical climatology patterns (Figure 4). No strong anomalies are found at the annual scale, though large year-to-year variability is seen in VPD, NINO3.4, and winter T_{air}. Monthly variability in Precip is also large. Finally, two variables show significant

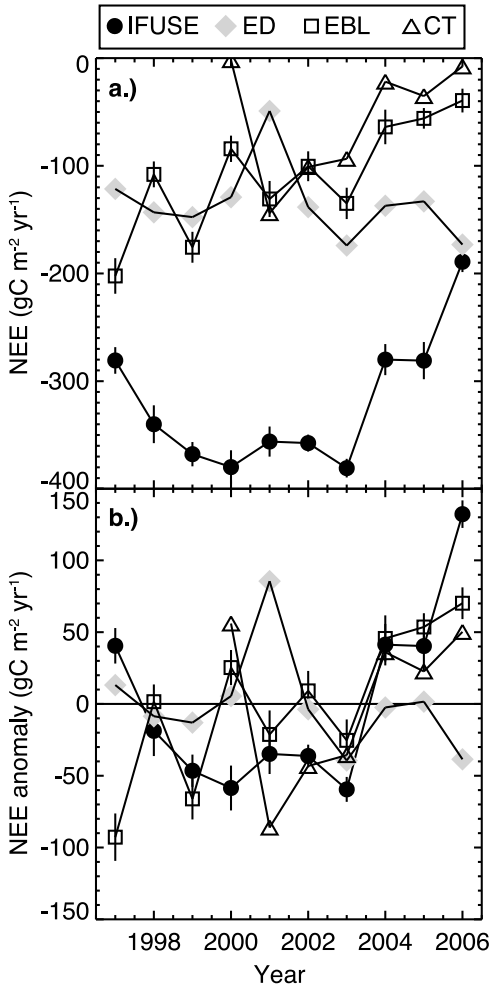

Figure 3. (a) Annual NEE and (b) annual NEE anomaly for each method. The 1-σ uncertainty for annual NEE is also shown. While there is large variation on magnitude of NEE, trends in NEE are coherent across several years and especially in the last 5 years of the record.

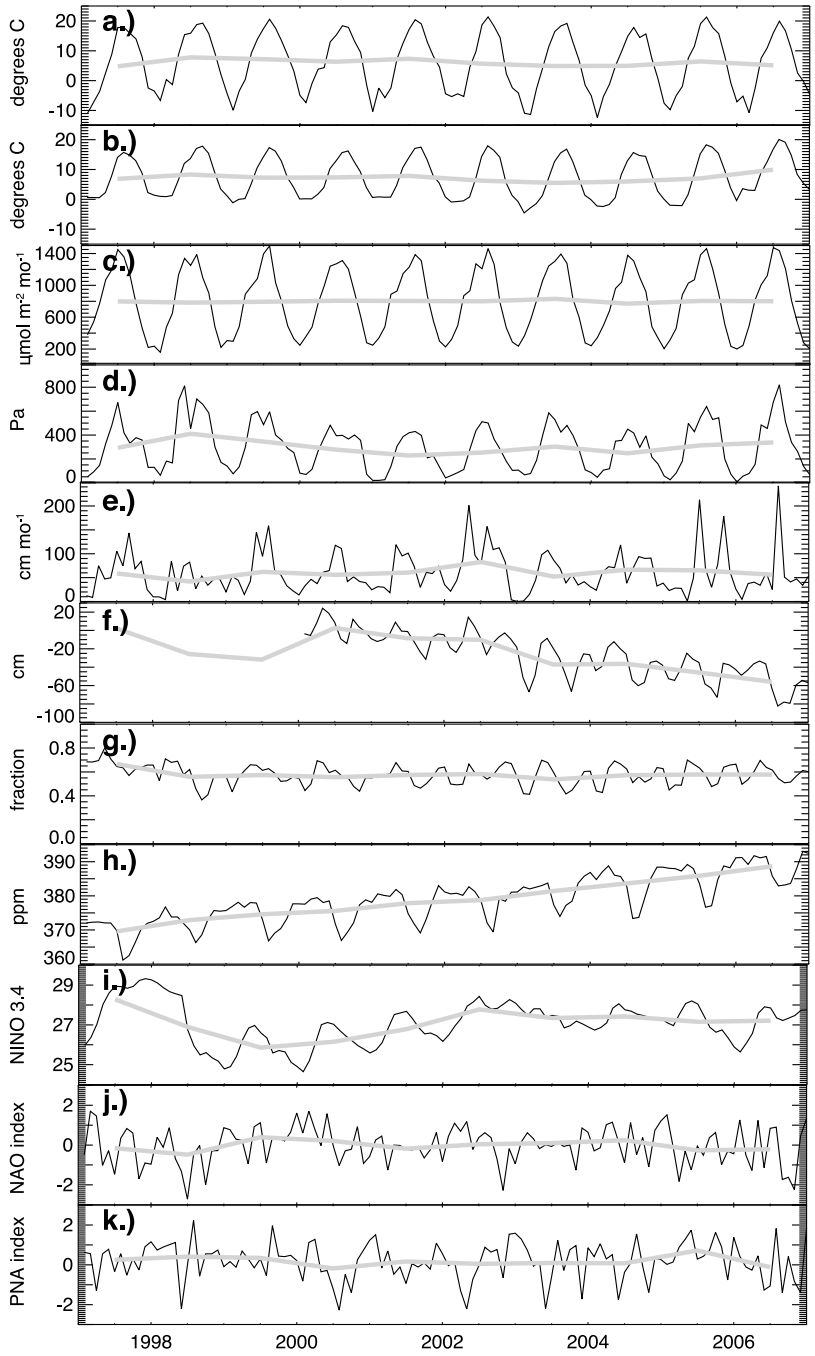

Figure 4. Monthly (black line) and annual average (gray line) climate variables: (a) T_{air}, (b) T_{soil}, (c) PAR, (d) VPD, (e) Precip, (f) Q_{table}, (g) Q_{soil}, (h) $[CO_2]$, (i) NINO3.4, (j) NAO, and (k) PNA. The strongest annual trends are seen in Q_{table} and $[CO_2]$.

linear trends, namely Q_{table} and $[CO_2]$. Q_{table} shows a declining (drying) trend that becomes stronger from 2003 to 2006. In contrast, the increasing trend of $[CO_2]$ is relatively steady, reflective of the dominance of global fossil fuel emissions on the secular trend in $[CO_2]$. While trends in Q_{table} are strong, they are only weakly correlated to Precip and a similar trend is not seen in Q_{soil}.

[45] The annual anomalies in climate have a wide range of correlation to annual anomalies in NEE (Table 3), at both no lag and 1 a lag timescales. However, only three variables show significant correlation based on a two-sided *t* test, Q_{table}, $[CO_2]$, and PNA. Two of these variables, Q_{table} and $[CO_2]$, are ones with trends in the time series. Interestingly, only $[CO_2]$ shows a significant correlation at lag 0, and with only one method (EBL), but at the 99% confidence level. All three variables have greater number of significant correlations at the lag 1 timescale. Lag 1 annual $[CO_2]$ is predictive for IFUSE and EBL at the 95% confidence level, while lag 1 annual Q_{table} is predictive for all methods except ED, at the 90% confidence level for EBL, 95% for IFUSE, and 99% for CT. In both of these cases, the sign of significant correlations are the same. In contrast, the significant

Table 3. Annual Correlation Coefficient Between Each Method NEE and Climate Variable at the Annual Timescale for Both No Lag and 1 Year Lag[a]

	Lag 0				Lag 1			
Control	IFUSE	ED	EBL	CT	IFUSE	ED	EBL	CT
T_{air}	−0.43	−0.08	0.43	−0.38	−0.34	−0.43	0.05	−0.16
T_{soil}	0.52	0.03	0.30	0.29	−0.38	0.16	−0.57	−0.37
PAR	−0.30	−0.10	−0.17	−0.35	0.16	0.10	0.18	−0.08
Precip	0.00	0.16	0.11	−0.24	0.03	−0.36	0.27	−0.07
VPD	0.14	−0.54	−0.03	0.55	−0.06	−0.10	−0.34	0.65
Q_{soil}	0.4	0.24	−0.48	0.02	−0.09	−0.24	−0.04	0.02
Q_{table}	−0.53	0.57	−0.53	−0.35	−0.66**	0.44	−0.61*	−0.96***
$[CO_2]$	0.50	−0.34	0.80***	0.42	0.75**	−0.27	0.71**	0.46
NAO	−0.38	−0.17	−0.18	0.21	−0.16	0.45	0.35	0.08
NINO3.4	0.42	−0.07	−0.06	−0.27	0.24	−0.56	0.07	0.09
PNA	0.01	0.12	−0.17	−0.17	0.48	−0.65*	0.28	0.72*

[a]Significance levels denoted by * ($p < 0.1$), ** ($p < 0.05$), and *** ($p < 0.01$). Only Q_{table}, $[CO_2]$, and PNA significantly explained IAV for at least one method.

correlations to lag 1 PNA for ED and CT at the 90% confidence level are of opposite sign, not surprising given the negative correlation of ED to the other three methods. Other variables with weaker, similar sign, but nonsignificant correlation for most methods include lag 0 T_{soil} and lag 0 Q_{table}.

[46] At the seasonal climate scale, a similar pattern emerges, though several other variables also become well correlated (Table 4). Seasonal lag 1 Q_{table} continues to show significant correlation for at least three methods in DJF, MAM, and SON, while seasonal lag 1 $[CO_2]$ has significant correlation only for IFUSE and EBL, but in all seasons, and also at lag 0 in DJF and JJA. JJA Lag 0 Q_{table} is also significantly correlated to IFUSE, EF, and EBL. Other climate factors with significant correlations for two methods include Lag 1 DJF T_{air}, Lag 1 DJF T_{soil} and Lag 1 MAM T_{soil}. While significant at the 90% level for only one method, TSON Lag 0 T_{soil} is unique for positive correlation across all four methods. Similarly, though with no significant correlations, Lag 0 and Lag 1 MAM PAR have negative relationships for all four methods. The relationship of spring and autumn forcing may be indicative of the role that growing season length has on interannual variability of NEE.

[47] Comparison of the climate variables to NEE anomalies for several of these variables reveals stronger consistency in the slope and intercepts of fits for top-down methods than bottom-up (Figure 5). The strength of the Lag 1 annual Q_{table} fit for IFUSE, EBL, and CT is particularly evident (Figure 5a), and it is also obvious that there is no significant relationship between Lag 1 Q_{table} and ED. Lag 1 annual CO_2 shows a similar finding, though with a stronger fit for ED and weaker fit for CT (Figure 5b). A nonlinear relationship to Lag 0 SON Tsoil is evident for ED, and potentially a similarly fit for EBL (Figure 5c). The fit to Lag 0 MAM PAR is driven primarily by an outlier of low spring PAR in 2004. Removal of this outlier significantly reduces the correlation for the top-down methods, with no change for IFUSE, and a slight increase for ED.

[48] The two strongest annual controls, Lag 1 annual $[CO_2]$, and lag 1 annual Q_{table}, along with the interactive effect of lag 1 annual $[CO_2]$ × lag 1 annual Q_{table} were fit using multivariate linear regression for all four models, and also a pooled model, where observations of NEE anomalies from each method were considered independent observations (Table 5). The model, while lacking in a large number of degrees of freedom (DOF), had strong correlations to observed NEE anomalies for IFUSE, EBL, and CT, with a weaker fit (but much larger DOF) to the pooled model, and the weakest fit to ED. Significant slopes of the model vary by method, with Q_{table} slope significant for IFUSE, CT, and the pooled model, while the $[CO_2]$ slope is only significant for IFUSE and CT. The interactive effect slope was highly significant ($p < 0.01$) for IFUSE, and strongly significant ($p < 0.05$) for the pooled model, but not significant for any other method. Oddly, none of the slopes are significant for EBL, though the overall model fit to NEE anomalies is good ($r^2 = 0.69$). Graphically (Figure 6), the strong relationship to CT and IFUSE is evident. Outliers on both ends drive the fit to EBL. The global fit for the four methods has a significant correlation ($r^2 = 0.84$, $p < 0.01$), suggesting that these two variables can explain much of the IAV of regional NEE over the time period studied.

4. Discussion

4.1. Coherence of Regional Fluxes

[49] While all four methods revealed a regional carbon sink with a similar magnitude of IAV, there was wide disagreement on the magnitude of NEE and generally weak coherence of IAV over the entire decade. Some of the disagreement in mean NEE, especially for CT, can be resolved by differences in nongrowing season fluxes, which are small in magnitude but persist for many months. Particularly with the case of IFUSE, the disagreement can be pinpointed to the large summer uptake. The rest of the disagreement appears to be related to the timing of the seasonal cycle, especially for spring green-up and fall leaf-out.

[50] Interannual variability of NEE continues to be difficult to estimate. The best that can be said from this study is that 1-σ IAV averaged to 48 g C m^{-2} yr^{-1} for the methods, but this reflected a wide range in terms of relative percentage of annual or seasonal NEE. This IAV is relatively small compared to other regions, reflective partially of the expected IAV for temperate midlatitude mesic mixed forests [*Stoy et al.*, 2009]. Surprisingly, regional IAV is smaller than many of the individual flux tower IAV suggesting that climate impacts on IAV at the ecosystem scale are not

Table 4. Correlation of Annual NEE for Each Method Against Seasonal Average Climate Variables[a]

	Lag 0				Lag 1			
Control	IFUSE	ED	EBL	CT	IFUSE	ED	EBL	CT
DJF								
T_{air}	−0.45	0.16	0.16	−0.04	−0.57	0.23	−0.76**	−0.72*
T_{soil}	0.37	0.21	0.00	0.14	−0.69**	0.14	−0.75**	−0.58
PAR	−0.14	0.15	−0.71**	−0.39	−0.04	0.14	0.25	0.01
Precip	−0.01	0.23	0.30	0.24	−0.03	0.12	0.29	−0.09
VPD	−0.37	−0.49	−0.27	0.49	−0.28	0.24	−0.35	0.34
Q_{soil}	0.32	0.26	−0.39	−0.21	−0.34	−0.27	−0.54	−0.33
Q_{table}	−0.38	0.62*	−0.45	−0.28	−0.69**	0.42	−0.63*	−0.93***
$[CO_2]$	0.57*	−0.29	0.82***	0.49	0.76**	−0.25	0.73**	0.44
MAM								
T_{air}	−0.26	0.02	0.13	0.40	−0.17	0.42	−0.20	0.03
T_{soil}	0.29	0.00	0.14	0.27	−0.6*	0.42	−0.65*	−0.42
PAR	−0.41	−0.13	−0.36	−0.40	−0.28	−0.11	−0.52	−0.18
Precip	−0.44	0.07	−0.18	−0.56	−0.48	−0.21	−0.22	−0.25
VPD	−0.21	−0.41	−0.16	0.44	−0.18	0.10	−0.35	0.46
Q_{soil}	0.27	−0.05	−0.47	0.56	−0.01	0.29	0.00	0.14
Q_{table}	−0.48	0.52	−0.48	−0.23	−0.67**	0.51	−0.62*	−0.95***
$[CO_2]$	0.54	−0.27	0.78***	0.46	0.73**	−0.21	0.75**	0.44
JJA								
T_{air}	−0.31	0.21	−0.09	−0.58	−0.02	−0.50	−0.06	0.07
T_{soil}	0.56*	−0.16	0.47	0.10	0.11	−0.56	−0.08	0.16
PAR	0.50	−0.2	0.14	−0.06	0.47	−0.51	0.60*	0.52
Precip	0.29	−0.17	−0.06	0.28	−0.05	−0.15	0.11	0.03
VPD	0.58*	−0.48	0.29	0.28	0.22	−0.55	−0.15	0.68*
Q_{soil}	0.19	−0.02	−0.28	0.71	−0.09	0.19	0.23	0.06
Q_{table}	−0.64**	0.55*	−0.61*	−0.49	−0.62*	0.40	−0.57	−0.92***
$[CO_2]$	0.56*	−0.38	0.78***	0.36	0.74**	−0.34	0.69**	0.54
SON								
T_{air}	−0.38	0.49	−0.24	−0.17	0.03	0.13	−0.01	0.23
T_{soil}	0.55*	0.19	0.51	0.47	0.36	0.04	0.03	0.04
PAR	−0.31	0.16	0.43	0.22	0.21	0.63*	0.25	−0.36
Precip	0.23	0.32	0.32	−0.06	0.74**	−0.52	0.53	0.22
VPD	0.01	−0.4	−0.19	0.78	0.03	0.19	−0.22	0.49
Q_{soil}	0.33	0.15	−0.11	−0.33	0.09	−0.67**	0.12	0.08
Q_{table}	−0.52	0.52	−0.50	−0.30	−0.64*	0.41	−0.63*	−0.95***
$[CO_2]$	0.49	−0.31	0.83***	0.39	0.77**	−0.3	0.64*	0.41

[a]Significance levels denoted by * ($p < 0.1$), ** ($p < 0.05$), and *** ($p < 0.01$). In addition to correlations seen in Q_{table} and $[CO_2]$ at annual scales, significant correlations are also seen with DJF T_{soil} and T_{air}, MAM T_{soil}, JJA PAR, SON PAR, Precip, and Q_{soil}.

strongly coherent (e.g., opposite climate-NEE relationships of wetlands and forests). Additionally, the regional IAV is small enough to be within the detection limits for the methods. The errors estimated for each model here are relatively conservative and do not include many of the known systematic errors in flux towers, boundary layer budgets, and inverse models. However, the number of significant relationships observed between IAV and climate variables suggests our estimates of IAV are significantly different from zero and reflect a modest sensitivity of regional NEE to climate.

[51] The magnitude of relative IAV (IAV/NEE) is smaller and more consistent among the bottom-up methods when compared to both annual and seasonal NEE, but the correlation of IAV is greater among the top-down methods. A similar finding has been seen in a continental-scale comparison of multiple top-down and bottom-up techniques [*Jacobson et al.*, 2008], suggesting that this finding is a general feature of the methods. True IAV for the region is likely somewhere in between, as top-down methods may be more likely to extrapolate errors in atmospheric observation and external forcing (e.g., fossil fuel emissions) into IAV, while bottom-up methods may be more likely to focus on capturing mean responses to short-timescale environmental forcing. Thus, model structural characterization is as important as climate forcing characterization for determining carbon cycle IAV and response to climatic forcing.

[52] Still, there are particular time periods where coherent anomalies in NEE are apparent among several methods. The first of these is 1998, which shows smaller NEE than 1999 for all methods. A large regional warm spring anomaly was present in 1998 [*Black et al.*, 2000], which likely affected both the timing of spring green-out and the rates of organic matter decomposition. Another coherent set is 2002–2004, where all four methods show neutral to greater uptake from 2002 to 2003, followed by a positive NEE anomaly in 2004. In a comparison of two flux tower sites in that period, *Desai et al.* [2005] noted coherence in NEE anomalies over that time period were driven strongly by summer moisture and precipitation anomalies, with 2003 the wettest of the triad and 2004 witnessing strong later summer drying.

[53] In the spring of 2001, the region suffered from a particularly large outbreak of forest tent caterpillar, leading to large-scale defoliation across the region in early summer, followed by late summer reflush [*Cook et al.*, 2008]. ED had this outbreak explicitly included as a disturbance, while the other models responded depended on the extent to which the observed calibration data (flux tower and/or atmospheric

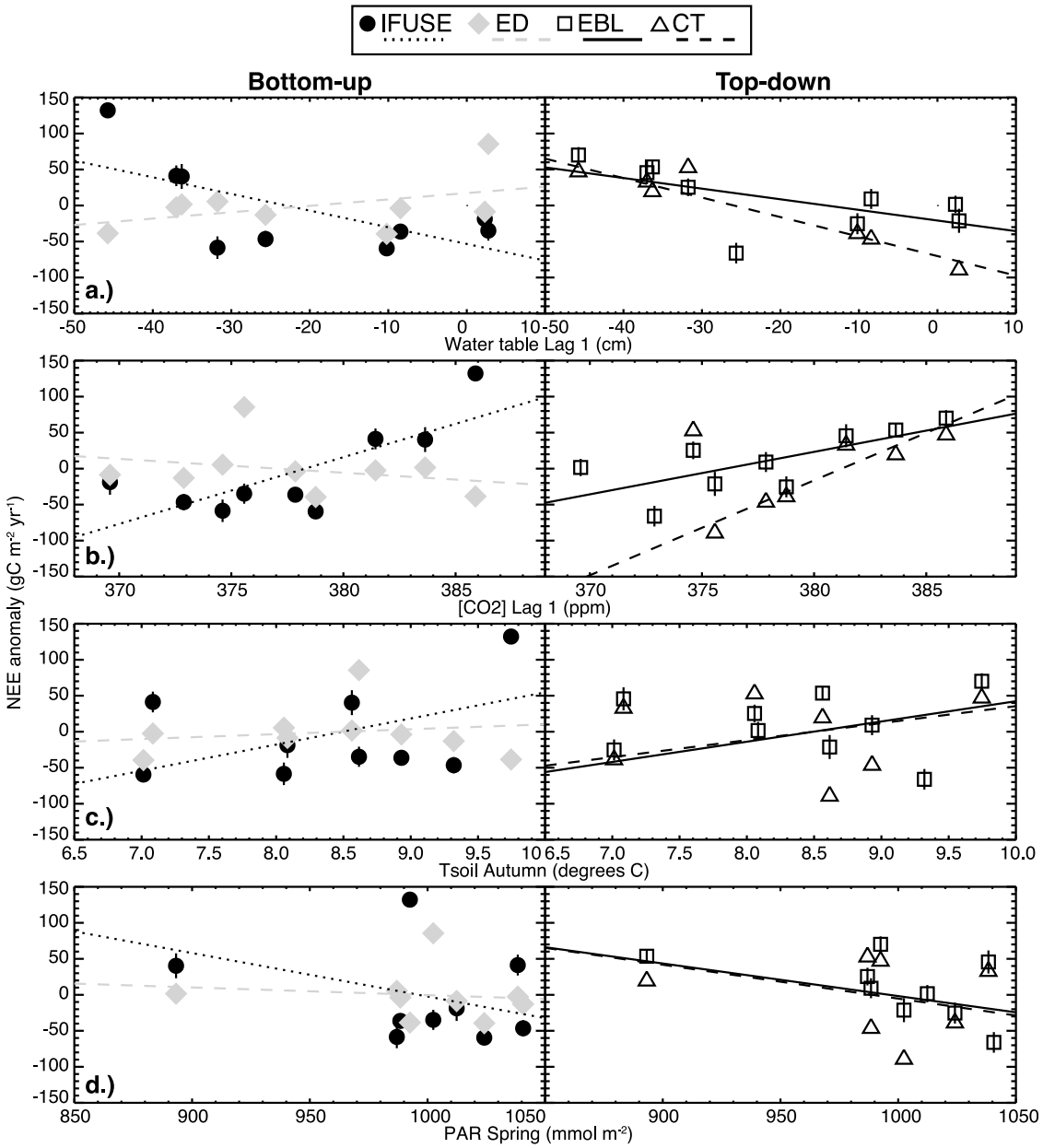

Figure 5. Scatterplot of annual NEE anomaly to (a) lag 1 year Q_{table}, (b) lag 1 year [CO_2], (c) SON Tsoil, and (d) MAM PAR for (left) bottom-up and (right) top-down methods. Top-down methods and IFUSE agree on slope of correlation, while ED generally differs.

CO_2) contained a signal of the outbreak. Anomalies for that year are not consistent. The bottom-up methods show a decline in NEE from the prior year and ED is strongly sensitive to this, while the top-down methods show greater uptake in 2001. This result suggests the need to better parameterize the effects of large-scale pest outbreaks on NEE.

[54] Finally, there is a trend of increasing (less uptake) NEE from 2003 to 2006 in all four methods, most strongly seen in IFUSE, and most weakly in ED (where the trend ends in 2005). This trend is particularly interesting as it drives much of the strong correlations found between climate variables and IAV. No strong climate forcing, beyond the finding for Q_{table}, appears to explain this trend and more work is needed to better characterize any apparent climate transition that is affecting regional NEE.

4.2. Uncertainties in Regional Flux

[55] Given the spread in NEE among the methods, especially those not captured by the apparently conservative estimate of uncertainty applied, it is worthwhile to characterize major sources of uncertainty for each method not included in the random error estimate. These are summarized below.

[56] The biggest shortcoming of IFUSE is the lack of flux tower replicates for all land cover and age classes [*Desai et al.*, 2008]. The strong growing season uptake in IFUSE is driven mainly by a couple of flux towers located in mature

Table 5. Least Squares Coefficients, Parameter Standard Error, Correlation, and Degrees of Freedom for Multivariate Regression of Annual NEE Against Lag 1 Annual $[CO_2]$, Q_{table}, and Q_{table} x $[CO_2]$[a]

Method	$[CO_2]$	Q_{table}	Q_{table} x $[CO_2]$	Intercept	r^2	DOF
IFUSE	4.7 +/− 1.4**	−1.2 +/− 0.40**	−0.44 +/− 0.061***	−30 +/− 6.1***	0.96	5
ED	0.63 +/− 3.9	0.99 +/− 1.1	0.048 +/− 0.17	1.3 +/− 16	0.21	5
EBL	3.4 +/− 2.9	−0.70 +/− 0.83	−0.19 +/− 0.18	−1.2 +/− 12	0.69	5
CT	−3.4 +/− 1.4*	−3.6 +/− 0.2***	0.091 +/− 0.064	1.2 +/− 3.1	0.99	3
Pooled	1.2 +/− 2.1	−0.97 +/− 0.56*	−0.18 +/− 0.091**	−10 +/− 8.6	0.35	30

[a]Significance levels of parameters denoted by * ($p < 0.1$), ** ($p < 0.05$), and *** ($p < 0.01$). Pooled model treats each method's NEE as an independent observation. Q_{table} parameter is significant for three models, while $[CO_2]$ and Q_{table} x $[CO_2]$ are significant for two models.

northern hardwood forests, the dominant class. There is some evidence that these towers are not representative of the mean NEE of mature forests in the region [*Desai et al.*, 2007]. Furthermore, wetlands and young forests are poorly represented among the flux towers in addition to having large classification error [*Maxa and Bolstad*, 2009]. Finally, the parameter estimation used in IFUSE, while tuned to capture IAV, does not allow parameters to vary annually, nor does ecosystem state in one year affect the next (quasi steady state ecosystem pools assumption). Thus the IAV represented is reflective only of input climate forcing.

[57] Similar to IFUSE, the ED model is also hampered by the lack of replicate observations. Unlike IFUSE, the lack of replicates in ED is over time not space. The version of ED used here is tuned to two cycles of Forest Inventory and Analysis (FIA) observations across the region, which are measured roughly once per decade. Thus, no information is available to constrain the climate-driven IAV in ED. The stochastic processes of competition and disturbance, which may be properly parameterized in the mean, but incorrectly simulated for any particular year, also drives the IAV in ED, though these random disturbances tends to average out over cohorts, so IAV is primarily dominated by climate. Finally, FIA does not provide information on belowground processes.

[58] Techniques to identify the fingerprint of regional biospheric flux in atmospheric tracer observations are not trivial and sensitive to assumptions made about error covariance, footprints, and models [*Dolman et al.*, 2009]. The EBL model relies on a synoptically averaged boundary layer budget based on observations in and above the boundary layer. *Helliker et al.* [2004] show that EBL NEE is sensitive to choice in number of synoptic cycles to average, screening criteria for precipitation, and estimation technique for mean vertical subsidence velocity, which can impart approximately 20% uncertainty in the EBL NEE. Additionally, the surface influence footprint of the EBL method is not clear. Estimates for some LaGrangian particle dispersion model footprint climatologies suggest a 90% influence footprint of roughly 10^5 km^2, smaller than that estimated by *Gloor et al.* [2001], but still larger than the region assumed by IFUSE and ED.

[59] Finally, CT is a global nested grid tracer-transport inverse model and as such suffers from uncertainty that any global model applied to a regional scale would [*Peters et al.*, 2007]. CT is designed so that an ecosystem model drives the temporal pattern of "fast" processes, while "slow" processes are tuned by weekly parameters against atmospheric CO_2 data, including those from the WLEF tower. The parameters are separated by ecoregion, and the study region's deciduous broadleaf forest region spans a large fraction of North America. Thus, while the near-field of CT around WLEF is likely to be well constrained by the WLEF observations, the large-scale parameters likely reflect larger-scale climate variability instead of exclusively local region forcing. Finally, tuning of these slow processes is also sensitive to proper specification of fossil fuel emissions and ocean fluxes. For example, the region around WLEF may be sensitive to influence from the Great Lakes (M. Uliasz, personal communication, 2009), which is weakly constrained in CT.

[60] While the uncertainties in regional flux methods all deserve further examination, the uncertainties in estimating the state of regional climate should also not be ignored. Climate forcing data analyzed in this study were derived from a number of point-based sources, which may not be regionally representative, especially for ones with high spatial variability (e.g., Precip, Q_{table}, Q_{soil}, T_{soil}). These observations also contain gaps due to instrumental failure and require filling by alternate data sources. Annual averages of climate forcing will be sensitive to systematic errors in observations and gap filling, which could weaken or generate false relationships between IAV and forcing. Well-

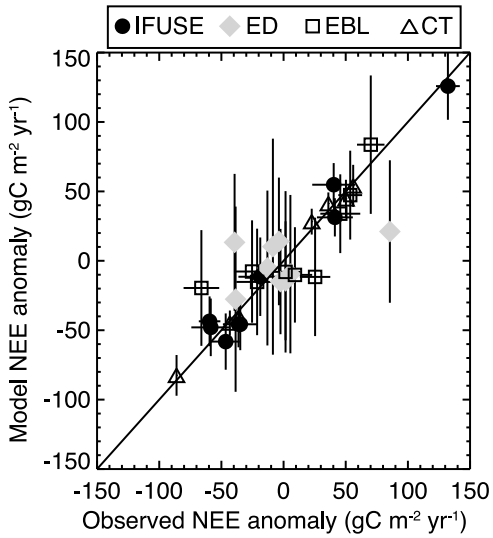

Figure 6. Fits of the individual nonpooled multivariate Q_{table} and $[CO_2]$ based model NEE anomaly against observed NEE anomaly for each method. Regression 90% confidence intervals and model 1-σ uncertainty are also shown. Fit has r^2 of 0.84 ($p < 0.01$) with 25 degrees of freedom. All but ED model are well explained by the multivariate model.

defined, gap-filled climate records for large regions continue to be a need for carbon cycle models.

4.3. Controls on Interannual Variability

[61] It is surprising that virtually none of the environmental forcing factors adequately explain the observed IAV across the four methods, outside of Q_{table} and $[CO_2]$. Moreover, the multiple linear regression pinpointed Q_{table} as the more important of the two factors. This is further evidenced when an estimate of global fossil fuel emissions is removed from the $[CO_2]$ anomaly, revealing only a weak correlation to the remaining $[CO_2]$ anomaly for all four methods. Additionally, three of four methods use $[CO_2]$ as a forcing factor in one form or another. Thus, the strong correlation to $[CO_2]$ appears to be spurious and driven primarily by the positive NEE trend in the last 4 years.

[62] So what to make of Q_{table}? There is some evidence to suggest that hydrology may be an important controlling factor of regional NEE, even in a mesic forest ecosystem [*Ricciuto et al.*, 2008; *Sulman et al.*, 2009], but it is surprising that a single-point observation of water table in a wetland is a strong predictor of regional IAV. *Sulman et al.* [2009] showed that while Q_{table} affects photosynthesis and decomposition in a wetland ecosystem, on net, they balance out, leading to no effect of Q_{table} on wetland NEE. More likely, Q_{table} is a better proxy for regional moisture availability than the point observation of precipitation or the poor spatial representation offered by Q_{soil}. Q_{table} was highly correlated to nearby bog level observations and precipitation at a site near the Q_{table} observation location. Similar to the drying trend in Q_{table}, a regional trend of long-term drying in northern Wisconsin, United States, is evident when weather station data are studied in aggregate [*Serbin and Kucharik*, 2009] or when Great Lakes water levels are analyzed [*Kratz et al.*, 2008]. Prior year autumn precipitation did show some correlation to NEE suggesting that late summer water stress carrying over into the following year may be one mechanism connecting carbon cycling and water availability, but the evidence here is weak and warrants more study. The regional drying trend, and the strength of the Q_{table}, especially as a lagged environmental predictor, provides a strong motivation for improving representation of hydrologic controls on carbon cycling in models.

[63] The level of carbon-water coupling in each method is quite different. EBL makes no assumption about hydrology and relies on variability in atmospheric CO_2. The same holds for CT, except that the bottom-up ecosystem model does contain moisture related functions for photosynthesis and respiration. IFUSE has functions to limit photosynthesis under moisture stress, while respiration is constrained indirectly via photosynthesis. ED has relatively weak moisture constraints, which might explain the different moisture response from the other three with respect to IAV. The results suggest that strong coupling of water and carbon is needed even in mesic regions to accurately simulate carbon cycle interannual variability. It should also be noted that models used here do not have energy cycles and at most had simplistic nutrient cycles. Feedbacks between moisture, energy balance, and nutrient cycles could not be investigated in this study.

[64] Though weaker in correlation, the roles of Spring PAR and Fall T_{soil} are likely representative of the importance of phenology as another strong region-wide control on growing season NEE, especially in forests [*Peñuelas et al.*, 2009; Desai, submitted manuscript, 2010]. Finally, no large-scale climate oscillation seemed to phase with regional IAV, except for Lag 1 PNA, whose significant correlations are of opposite sign for ED and CT. Still, PNA, associated with fluctuations of the East Asian jet stream, may serve as an indicator of larger-scale precipitation variability in the upper Midwest, which tends to be below average when PNA is positive.

[65] These findings for climatic controls on regional flux do have some agreement with an analysis of the eddy covariance fluxes measured at the WLEF tower, which sample a 5–10 km fetch around the tower [*Ricciuto et al.*, 2008]. *Ricciuto et al.* [2008] found no strong correlation between temperature and annual NEE, unless NEE was subset for night, suggesting temperature has opposing but equal effects on respiration and photosynthesis. In contrast, a negative correlation was found between NEE and Q_{soil}, once again highlighting a previously underappreciated role of hydrology in the carbon balance of boreal transition forests. Other factors such as plant water balance [*Law et al.*, 2002], nitrogen cycling [*Magnani et al.*, 2007], and disturbance dynamics [*Gough et al.*, 2008] have been shown to be controllers of IAV and also deserve more examination in relation to the regional IAV quantified in this study. Additionally, ecosystem rebound after stress may leave a multi-year fingerprint on NEE, something that is difficult to test even with a decade-long data set, highlighting the need for more long-term observations of regional NEE.

5. Conclusions

[66] There have been only limited comparisons of regional-scale carbon fluxes based on top-down atmospheric and bottom-up ecosystem upscaling approaches, and they have rarely been studied for interannual variability and climatic controls. The results from this study revealed that four independent methods, all showing carbon sinks, diverge on magnitude of NEE while showing some coherence in interannual variability, especially over subsets of the time period. The lack of convergence in regional NEE and the lack of full understanding of climatic controls on IAV severely limits our ability to accurately assess future contributions of terrestrial ecosystems to atmospheric CO_2 and climatic change.

[67] While there did not appear to be an exceptionally strong predictor of regional IAV, the surprising role of lagged hydrologic controls over regional IAV highlights the need to better incorporate and test hydrologic processes and coupled water-carbon cycles in current generation carbon-climate models. As it is becoming more apparent that terrestrial carbon cycling is characterized by a range of low-frequency modes of variability [*Stoy et al.*, 2009], continued analysis of lagged environmental oscillations and trends will be key to better prediction of carbon cycle variability and its impact on future climate change. Our results suggest that improved representation of carbon-water relationships, incorporation of wetland processes in ecosystem models, and continued quantification of model uncertainty and top-down/bottom-up model intercompari-

son all are likely to help improve predictions of the impacts of climate change to ecosystem biogeochemistry.

[68] **Acknowledgments.** This work could not have been done without the support of the many investigators, students, and technicians associated with the Chequamagon Ecosystem-Atmosphere Study (ChEAS), B. Cook of NASA Goddard Space Flight Center, R. Teclaw and D. Baumann of the U.S. Forest Service (USFS) Northern Research Station, R. Strand, chief engineer at WLEF, of the Wisconsin Education Communications Board (ECB), W. Peters and A. Jacobson of the NOAA ESRL CarbonTracker team, and M. Albani for ED North America development. This work was supported by the Department of Energy (DOE) Office of Biological and Environmental Research (BER) National Institute for Climatic Change Research (NICCR) Midwestern Region subagreement 050516Z19.

References

Ahl, D. E., S. T. Gower, and M. K. White (2005), Life cycle inventories of roundwood production in northern Wisconsin: Inputs into an industrial forest carbon budget, *For. Ecol. Manage.*, *219*, 13–28, doi:10.1016/j.foreco.2005.08.039.

Ahmadav, R., C. Gerbig, R. Kretschmer, S. Körner, C. Rödenbeck, P. Bousquet, and M. Ramonet (2009), Comparing high resolution WRF-VPRM simulations and two global CO_2 transport models with coastal tower measurements of CO_2, *Biogeosciences*, *6*, 807–817.

Albani, M., D. Medvigy, G. C. Hurtt, and P. R. Moorcroft (2006), The contributions of land-use change, CO_2 fertilization, and climate variability to the eastern US carbon sink, *Global Change Biol.*, *12*, 2370–2390, doi:10.1111/j.1365-2486.2006.01254.x.

Bakwin, P. S., P. P. Tans, D. F. Hurst, and C. Zhao (1998), Measurements of carbon dioxide on very tall towers: Results of the NOAA/CMDL program, *Tellus, Ser. B*, *50*, 401–415.

Bakwin, P. S., K. J. Davis, C. Yi, S. C. Wofsy, J. W. Munger, L. Haszpra, and Z. Barcza (2004), Regional carbon dioxide fluxes from mixing ratio data, *Tellus, Ser. B*, *56*, 301–311.

Betts, A. K., B. R. Helliker, and J. A. Berry (2004), Coupling between CO_2, water vapor, temperature and radon and their fluxes in an idealized equilibrium boundary layer over land, *J. Geophys. Res.*, *109*, D18103, doi:10.1029/2003JD004420.

Black, T. A., W. J. Chen, A. G. Barr, M. A. Arain, Z. Chen, Z. Nesic, E. H. Hogg, H. H. Neumann, and P. C. Yang (2000), Increased carbon sequestration by a boreal deciduous forest in years with a warm spring, *Geophys. Res. Lett.*, *27*(9), 1271–1274, doi:10.1029/1999GL011234.

Blankinship, J. C., D. A. Riveros-Iregui, and A. R. Desai (2008), NCAR Advanced Study Program students "method-hop" their way to regional biogeochemistry, *Bull. Am. Meteorol. Soc.*, *89*(10), 1571–1573, doi:10.1175/2008BAMS2615.1.

Bolstad, P. V., K. J. Davis, J. G. Martin, and B. D. Cook (2004), Component and whole-system respiration in northern deciduous forest stands, *Tree Physiol.*, *24*, 493–504.

Bonan, G. B. (2008), Forests and climate change: Forcings, feedbacks, and the climate benefits of forests, *Science*, *320*(5882), 1444–1449, doi:10.1126/science.1155121.

Bousquet, P., P. Peylin, P. Ciais, C. Le Quéré, P. Friedlingstein, and P. P. Tans (2000), Regional changes in carbon dioxide fluxes of land and oceans since 1980, *Science*, *290*(5495), 1342, doi:10.1126/science.290.5495.1342.

Braswell, B. H., B. Sacks, E. Linder, and D. S. Schimel (2005), Estimating ecosystem process parameters by assimilation of eddy flux observations of NEE, *Global Change Biol.*, *11*, 335–355, doi:10.1111/j.1365-2486.2005.00897.x.

Chen, B., J. M. Chen, G. Mo, T. A. Black, and D. E. J. Worthy (2008), Comparison of regional carbon flux estimates from CO_2 concentration measurements and remote sensing based footprint integration, *Global Biogeochem. Cycles*, *22*, GB2012, doi:10.1029/2007GB003024.

Chen, J., K. J. Davis, and T. P. Meyers (2008), Ecosystem-atmosphere carbon and water cycling in the upper Great Lakes region, *Agric. For. Meteorol.*, *148*, 155–157, doi:10.1016/j.agrformet.2007.08.016.

Chen, J. M., B. Chen, and P. P. Tans (2007), Deriving daily carbon fluxes from hourly CO_2 mixing ratios measured on the WLEF tall tower: An upscaling methodology, *J. Geophys. Res.*, *112*, G01015, doi:10.1029/2006JG000280.

Cleugh, H. A., M. R. Raupach, P. R. Briggs, and P. A. Coppin (2004), Regional-scale heat and water vapour fluxes in an agricultural landscape: An evaluation of CBL budget methods at OASIS, *Boundary Layer Meteorol.*, *110*, 99–137, doi:10.1023/A:1026096711297.

Cohen, W. B., M. E. Harmon, D. O. Wallin, and M. Fiorella (1996), Two decades of carbon flux from forests of the Pacific Northwest, *BioScience*, *46*(11), 836–844, doi:10.2307/1312969.

Cook, B. D., P. V. Bolstad, J. G. Martin, F. A. Heinsch, K. J. Davis, W. Wang, A. R. Desai, and R. M. Teclaw (2008), Using light-use and production efficiency models to predict forest production and carbon exchange during canopy disturbance events, *Ecosystems*, *11*, 26–44, doi:10.1007/s10021-007-9105-0.

Davis, K. J., P. S. Bakwin, C. Yi, B. W. Berger, C. Zhao, R. M. Teclaw, and J. G. Isebrands (2003), The annual cycles of CO_2 and H_2O exchange over a northern mixed forest as observed from a very tall tower, *Global Change Biol.*, *9*(9), 1278–1293, doi:10.1046/j.1365-2486.2003.00672.x.

Denmead, O. T., M. R. Raupach, F. X. Dunin, H. A. Cleugh, and R. Leuning (1996), Boundary layer budgets for regional estimates of scalar fluxes, *Global Change Biol.*, *2*, 255–264, doi:10.1111/j.1365-2486.1996.tb00077.x.

Desai, A. R., P. V. Bolstad, B. D. Cook, K. J. Davis, and E. V. Carey (2005), Comparing net ecosystem exchange of carbon dioxide between an old-growth and mature forest in the upper Midwest, USA, *Agric. For. Meteorol.*, *128*(1–2), 33–55, doi:10.1016/j.agrformet.2004.09.005.

Desai, A. R., P. R. Moorcroft, P. V. Bolstad, and K. J. Davis (2007), Regional carbon fluxes from a biometrically constrained dynamic ecosystem model: Impact of disturbance, CO_2 fertilization and heterogeneous land cover, *J. Geophys. Res.*, *112*, G01017, doi:10.1029/2006JG000264.

Desai, A. R., et al. (2008), Influence of vegetation and seasonal forcing on carbon dioxide fluxes across the Upper Midwest, USA: Implications for regional scaling, *Agric. For. Meteorol.*, *148*(2), 288–308, doi:10.1016/j.agrformet.2007.08.001.

Dolman, A. J., C. Gerbig, J. Noilhan, C. Sarrat, and F. Miglietta (2009), Detecting regional variability in sources and sinks of carbon dioxide: A synthesis, *Biogeosciences*, *6*, 1015–1026.

Friedlingstein, P., et al. (2006), Climate-carbon cycle feedback analysis, results from the C4MIP model intercomparison, *J. Clim.*, *19*, 3337–3353, doi:10.1175/JCLI3800.1.

Gloor, M., P. Bakwin, D. Hurst, L. Lock, R. Draxler, and P. Tans (2001), What is the concentration footprint of a tall tower?, *J. Geophys. Res.*, *106*, 17,831–17,840, doi:10.1029/2001JD900021.

Goodale, C. L., et al. (2002), Forest carbon sinks in the Northern Hemisphere, *Ecol. Appl.*, *12*, 891–899, doi:10.1890/1051-0761(2002)012[0891:FCSITN]2.0.CO;2.

Gough, C., C. Vogel, H.-P. Schmid, and P. S. Curtis (2008), Controls on annual forest carbon storage: Lessons from the past and predictions for the future, *BioScience*, *58*(7), 609–622, doi:10.1641/B580708.

Gurney, K. R., et al. (2002), Towards robust regional estimates of CO_2 sources and sinks using atmospheric transport models, *Nature*, *415*(6872), 626–630, doi:10.1038/415626a.

Helliker, B. R., J. A. Berry, A. K. Betts, K. J. Davis, J. Miller, A. S. Denning, P. Bakwin, J. Ehleringer, M. P. Butler, and D. M. Ricciuto (2004), Estimates of net CO_2 flux by application of equilibrium boundary layer concepts to CO_2 and water vapor measurements from a tall tower, *J. Geophys. Res.*, *109*, D20106, doi:10.1029/2004JD004532.

Hurwitz, M. D., D. M. Ricciuto, K. J. Davis, W. Wang, C. Yi, M. P. Butler, and P. S. Bakwin (2004), Advection of carbon dioxide in the presence of storm systems over a northern Wisconsin forest, *J. Atmos. Sci.*, *61*, 607–618, doi:10.1175/1520-0469(2004)061<0607:TOCDIT>2.0.CO;2.

Jacobson, A. R., W. M. Post, and D. N. Huntzinger (2008), Comparing the interannual variability of forward and inverse models, *Eos Trans. AGU*, *89*(53), Fall Meet. Suppl., Abstract B54A–06.

Kicklighter, D. W., J. M. Melillo, W. T. Peterjohn, E. B. Rastetter, A. D. McGuire, P. A. Steudler, and J. D. Aber (1994), Aspects of spatial and temporal aggregation in estimating regional carbon dioxide fluxes from temperate forest soils, *J. Geophys. Res.*, *99*(D1), 1303–1315, doi:10.1029/93JD02964.

Kratz, T. K., T. K. Kratz, E. C. Lamon, and C. E. Sellinger (2008), Lake level coherence supports common driver, *Eos Trans. AGU*, *89*(41), 389, doi:10.1029/2008EO410001.

Kuck, L. R., et al. (2000), Measurements of landscape-scale fluxes of carbon dioxide in the Peruvian Amazon by vertical profiling through the atmospheric boundary layer, *J. Geophys. Res.*, *105*(D17), 22,137–22,146, doi:10.1029/2000JD900105.

Law, B. E., et al. (2002), Environmental controls over carbon dioxide and water vapor exchange of terrestrial vegetation, *Agric. For. Meteorol.*, *113*, 97–120, doi:10.1016/S0168-1923(02)00104-1.

Leuning, R., M. R. Raupach, P. A. Coppin, H. A. Cleugh, P. Isaac, O. T. Denmead, F. X. Dunin, S. Zegelin, and J. Hacker (2004), Spatial and temporal variations in fluxes of energy, water vapour and carbon dioxide during OASIS 1994 and 1995, *Boundary Layer Meteorol.*, *110*, 3–38, doi:10.1023/A:1026028217081.

Levy, P. E., A. Grelle, A. Lindroth, M. Molder, P. G. Jarvis, B. Kruijt, and J. B. Moncrieff (1999), Regional-scale CO_2 fluxes over central Sweden by a boundary layer budget method, *Agric. For. Meteorol.*, *99*, 169–180, doi:10.1016/S0168-1923(99)00096-9.

Lin, J., C. Gerbig, S. Wofsy, A. Andrews, B. Daube, C. Grainger, B. Stephens, P. Bakwin, and D. Hollinger (2004), Measuring fluxes of trace gases at regional scales by Lagrangian observations: Application to the CO_2 Budget and Rectification Airborne (COBRA) study, *J. Geophys. Res.*, *109*, D15304, doi:10.1029/2004JD004754.

Lloyd, J., et al. (2001), Vertical profiles, boundary layer budgets, and regional flux estimates for CO_2 and its $^{13}C/^{12}C$ ratio and for water vapor above a forest/bog mosaic in central Siberia, *Global Biogeochem. Cycles*, *15*(2), 267–284, doi:10.1029/1999GB001211.

Luo, Y., E. Weng, X. Wu, C. Gao, X. Zhou, and L. Zhang (2009), Parameter identifiability, constrain, and equifinality in data assimilation with ecosystem models, *Ecol. Appl.*, *19*, 571–574, doi:10.1890/08-0561.1.

Magnani, F., et al. (2007), The human footprint in the carbon cycle of temperate and boreal forests, *Nature*, *447*, 848–850, doi:10.1038/nature05847.

Mahadevan, P., S. C. Wofsy, D. M. Matross, X. Xiao, A. L. Dunn, J. C. Lin, C. Gerbig, J. W. Munger, V. Y. Chow, and E. W. Gottlieb (2008), A satellite-based biosphere parameterization for net ecosystem CO_2 exchange: Vegetation photosynthesis and respiration model (VPRM), *Global Biogeochem. Cycles*, *22*, GB2005, doi:10.1029/2006GB002735.

Matross, D., A. Andrews, and M. Pathmathevan (2006), Estimating regional carbon exchange in New England and Quebec by combining atmospheric, ground-based and satellite data, *Tellus, Ser. B*, *58*, 344–358.

Maxa, M., and P. V. Bolstad (2009), Mapping northern wetlands with high resolution satellite images and LiDAR, *Wetlands*, *29*, 248–260, doi:10.1672/08-91.1.

Metropolis, N., and S. Ulam (1949), The Monte Carlo method, *J. Am. Stat. Assoc.*, *44*, 335–341, doi:10.2307/2280232.

Moorcroft, P. R. (2006), How close are we to a predictive science of the biosphere?, *Trends Ecol. Evol.*, *121*, 400–407, doi:10.1016/j.tree.2006.04.009.

Moorcroft, P. R., G. C. Hurtt, and S. W. Pacala (2001), A method for scaling vegetation dynamics: The ecosystem demography model (ED), *Ecol. Monogr.*, *71*, 557–585.

Pacala, S. W., et al. (2001), Consistent land- and atmosphere-based U.S. carbon sink estimates, *Science*, *292*, 2316–2320, doi:10.1126/science.1057320.

Papale, D., and A. Valentini (2003), A new assessment of European forests carbon exchange by eddy fluxes and artificial neural network spatialization, *Global Change Biol.*, *9*, 525–535, doi:10.1046/j.1365-2486.2003.00609.x.

Peñuelas, J., T. Rutishauser, and I. Filella (2009), Phenology feedbacks on climate change, *Science*, *324*(5929), 887–888, doi:10.1126/science.1173004.

Peters, W., et al. (2005), An ensemble data assimilation system to estimate CO_2 surface fluxes from atmospheric trace gas observations, *J. Geophys. Res.*, *110*, D24304, doi:10.1029/2005JD006157.

Peters, W., et al. (2007), An atmospheric perspective on North American carbon dioxide exchange: CarbonTracker, *Proc. Natl. Acad. Sci. U. S. A.*, *104*(48), 18,925–18,930, doi:10.1073/pnas.0708986104.

Peylin, P., P. Bousquet, C. Le Quéré, S. Sitch, P. Friedlingstein, G. McKinley, N. Gruber, P. Rayner, and P. Ciais (2005), Multiple constraints on regional CO_2 flux variations over land and oceans, *Global Biogeochem. Cycles*, *19*, GB1011, doi:10.1029/2003GB002214.

Raupach, M. R., O. T. Denmead, and F. X. Dunin (1992), Challenges in linking atmospheric CO_2 concentrations to fluxes at local and regional scales, *Aust. J. Bot.*, *40*, 697–716, doi:10.1071/BT9920697.

Ricciuto, D. M., M. P. Butler, K. J. Davis, B. D. Cook, P. S. Bakwin, A. Andrews, and R. M. Teclaw (2008), Causes of interannual variability in ecosystem–atmosphere CO_2 exchange in a northern Wisconsin forest using a Bayesian model calibration, *Agric. For. Meteorol.*, *148*(2), 309–327, doi:10.1016/j.agrformet.2007.08.007.

Riley, W. J., S. C. Biraud, M. S. Torn, M. L. Fischer, D. P. Billesbach, and J. A. Berry (2009), Regional CO2 and latent heat surface fluxes in the Southern Great Plains: Measurements, modeling, and scaling, *J. Geophys. Res.*, *114*, G04009, doi:10.1029/2009JG001003.

Running, S. W. (2008), Ecosystem disturbance, carbon, and climate, *Science*, *321*, 652–653, doi:10.1126/science.1159607.

Serbin, S. P., and C. J. Kucharik (2009), Spatiotemporal mapping of temperature and precipitation for the development of a multidecadal climatic dataset for Wisconsin, *J. Appl. Meteorol. Climatol.*, *48*, 742–757, doi:10.1175/2008JAMC1986.1.

Stoy, P. C., et al. (2009), Biosphere-atmosphere exchange of CO_2 in relation to climate: A cross-biome analysis across multiple time scales, *Biogeosciences*, *6*, 2297–2312.

Styles, J. M., J. Lloyd, D. Zolotoukhine, K. A. Lawton, N. Tchebakova, R. J. Francey, A. Arneth, D. Salamakho, O. Kolle, and E. -D. Schulze (2002), Estimates of regional surface carbon dioxide exchange and carbon and oxygen isotope discrimination during photosynthesis from concentration profiles in the atmospheric boundary layer, *Tellus, Ser. B*, *54*, 768–783.

Sulman, B. N., A. R. Desai, B. D. Cook, N. Saliendra, and D. S. Mackay (2009), Contrasting carbon dioxide fluxes between a drying shrub wetland in Northern Wisconsin, USA, and nearby forests, *Biogeosciences*, *6*, 1115–1126.

Wang, W. G., K. J. Davis, B. D. Cook, C. Yi, M. P. Butler, D. M. Ricciuto, and P. S. Bakwin (2007), Estimating daytime CO_2 fluxes over a mixed forest from tall tower mixing ratio measurements, *J. Geophys. Res.*, *112*, D10308, doi:10.1029/2006JD007770.

Wofsy, S. C., and R. C. Harriss (2002), The North American Carbon Program (NACP), report of the NACP Committee of the U.S. Interagency Carbon Cycle Science Program, U.S. Global Change Res. Program, Washington, D. C.

Xiao, J., et al. (2008), Estimation of net ecosystem carbon exchange for the conterminous United States by combining MODIS and AmeriFlux data, *Agric. For. Meteorol.*, *148*(11), 1827–1847, doi:10.1016/j.agrformet.2008.06.015.

A. E. Andrews, Earth System Research Laboratory, National Oceanic and Atmospheric Administration, Boulder, CO 80305, USA.

J. A. Berry, Carnegie Institution of Washington, Stanford University, Stanford, CA 94305, USA.

A. R. Desai, Department of Atmospheric and Oceanic Sciences, University of Wisconsin-Madison, AOSS 1549, 1225 W. Dayton St., Madison, WI 53706, USA. (desai@aos.wisc.edu)

B. R. Helliker, Department of Biology, University of Pennsylvania, Philadelphia, PA 19104, USA.

P. R. Moorcroft, Department of Organismic and Evolutionary Biology, Harvard University, Cambridge, MA 02138, USA.